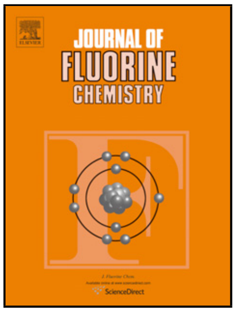

Title: Synthesis of UF_4 and ThF_4 by HF gas fluorination and re-determination of the UF_4 melting point

Authors: Pavel Souček, Ondřej Beneš, Benoit Claux, Elisa Capelli, Michel Ougier, Václav Tyrpekl, Jean-Francois Vigier, Rudy J.M. Konings

PII: S0022-1139(17)30169-0
DOI: http://dx.doi.org/doi:10.1016/j.jfluchem.2017.05.011
Reference: FLUOR 8988

To appear in: *FLUOR*

Received date: 25-4-2017
Revised date: 19-5-2017
Accepted date: 19-5-2017

Please cite this article as: Pavel Souček, Ondřej Beneš, Benoit Claux, Elisa Capelli, Michel Ougier, Václav Tyrpekl, Jean-Francois Vigier, Rudy J.M.Konings, Synthesis of UF4 and ThF4 by HF gas fluorination and re-determination of the UF4 melting point, Journal of Fluorine Chemistryhttp://dx.doi.org/10.1016/j.jfluchem.2017.05.011

Synthesis of UF_4 and ThF_4 by HF gas fluorination and re-determination of the UF_4 melting point

Pavel Souček*, Ondřej Beneš, Benoit Claux, Elisa Capelli, Michel Ougier,
Václav Tyrpekl, Jean-Francois Vigier and Rudy J. M. Konings

European Commission, Joint Research Centre, Postfach 2340, 76125 Karlsruhe, Germany

** Corresponding author, E-mail: Pavel.Soucek@ec.europa.eu, phone: +49-7247-951124*

Graphical abstract

Pure UF_4 and ThF_4 were synthesised using HF gas fluorination of the respective oxides and characterised by X-ray diffraction and differential scanning calorimetry. For the first time, the melting point of UF_4 was determined directly by a calorimetric technique using a pure sample and was found at a temperature of 1034.7 ± 3°C. A specially designed facility for synthesis of the actinide fluorides using HF gas is described. It consists of a glove box kept under a purified argon atmosphere, a high temperature horizontal fluorination reactor and a HF supply gas line connected to the glove box. The work demonstrated the capability of the installation to prepare very pure actinide fluorides sufficient for thermodynamic and electrochemical measurements, which is a very important step in the molten salt reactor fuel cycle safety assessment.

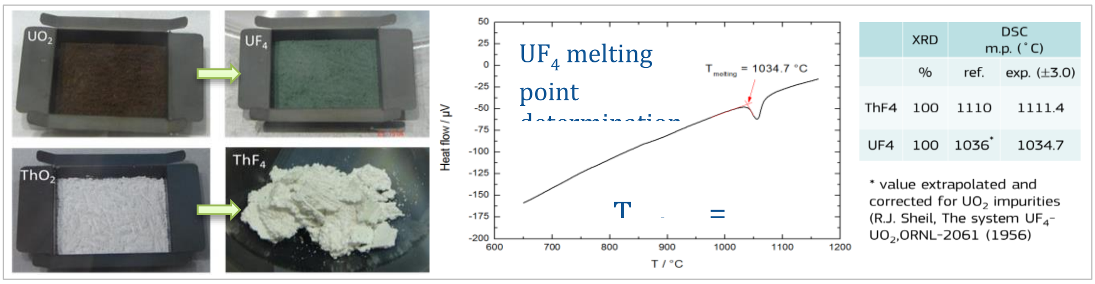

	XRD	DSC m.p. (°C)	
	%	ref.	exp. (±3.0)
ThF4	100	1110	1111.4
UF4	100	1036*	1034.7

* value extrapolated and corrected for UO_2 impurities (R.J. Sheil, The system UF_4-UO_2,ORNL-2061 (1956)

Pictogram source file – requested final size

Highlights

- UF_4 and ThF_4 were synthesised by HF gas fluorination of specially prepared UO_2 and ThO_2 powders with high specific surfaces.
- The prepared UF_4 and ThF_4 were characterised by X-ray diffraction and differential scanning calorimetry and found phase pure.
- For the first time, the melting point of UF_4 was determined directly by a calorimetric technique on a pure sample.
- A European-unique facility for synthesis of actinide fluorides using HF gas was designed, installed and proven efficient.
- The work demonstrated capability of the installation to prepare actinide fluorides with purity >99%.

Abstract

Basic thermodynamic and electrochemical data of pure actinide fluorides and their mixtures are required for the design and safety assessment of any presently studied molten salt reactor concept based on molten fluoride salt fuel. Since the actinide fluorides are usually not produced commercially, they have to be prepared from the available input materials, typically oxides. In this work, a specially designed facility for synthesis of pure actinide fluorides using pure HF gas is described, as well as a complete procedure of synthesis and characterisation of pure UF_4 and ThF_4. The fluorination installation consists of a glove box kept under a purified argon atmosphere, a high temperature horizontal fluorination reactor and a HF supply gas line connected to the glove box. The fluorides were synthesised from high specific surface oxides prepared from the respective oxalates by low temperature calcination. The fluorination was partly stationary and partly in a HF gas flow, based on a heterogeneous powder-gas reaction at high temperatures. The products were characterised by X-ray diffraction and differential scanning calorimetry, which confirmed high purity products obtained by this method. Moreover, the melting point of UF_4 was revised using a pure sample and a new value is suggested.

Keywords: Molten Salt Reactor, actinide fluorides, UF_4 synthesis, ThF_4 synthesis, fluorination, hydrogen fluorine

1. Introduction

The molten salt reactor (MSR) concept is based on a liquid fuel circulating through the reactor core and vessel, serving in the same time as a primary coolant. The fuel is composed of a molten halide salt where the fissile / fertile material is dissolved in the form of an actinide halide, while both fluoride and chloride are being investigated. The original concept of a reactor with graphite moderator providing a thermal neutron spectrum was developed in Oak Ridge National Laboratory, USA, where an intensive research was carried out in the 1960s on power reactor designs as either simple converters or breeder reactors utilising the ^{232}Th-^{233}U cycle [1, 2]. Since 2002, the MSR has been included to the Generation IV initiative studying six selected innovative future power reactor concepts [3, 4]. It positively increased interest in this field and several reactor designs were proposed and presently being studied worldwide, based on the thermal reactor system [5], but also, e.g., accelerator-driven sub-critical reactors [6-8] or transuranium elements (TRU) burner [9].

The concept intensively studied in Europe is the Molten Salt Fast Reactor (MSFR), based on a non-moderated epi-thermal neutron spectrum with an initial fuel salt composed of LiF (77.5 mol.%),ThF_4 (20.0 mol.%) and UF_4 (2.5 mol.%) [10]. U is present as a fissile material, Th as a fertile material and the composition is close to the eutectic point of the pseudo-binary mixture with fixed UF_4 composition. The main advantages of the MSFR with homogeneous core are analogous to those generally arising from use of a liquid molten salt fuel, i.e., large negative temperature coefficient of reactivity due to a high thermal expansion, low atmospheric pressure in the core during the operation, possibility of continuous fission-product removal with relaxed (1-3 years) removal time for soluble fission products via physical and pyrochemical processes which brings a flexibility in the fuel cycle, no transport and fabrication of new fuel elements etc. [3, 11]. There is no solid moderator in the core of the MSFR, eliminating the graphite lifespan issues.

Basic thermodynamic and electrochemical data of pure actinide fluorides and their mixtures are required for the design and safety assessment of any MSR concept based on molten fluoride salt fuel. Since the actinide fluorides are usually not produced commercially, they have to be prepared from the available input materials, typically oxides. In this work, the main attention is given to the synthesis and characterisation of pure UF_4 and ThF_4 as the key fuel constituents of MSFR. Based on the literature survey presented below, it was decided to use a direct hydrofluorination of both actinides oxides, while a special attention was paid to a preparation of input material. In both cases, a high specific surface oxide powder was prepared from the respective oxalates. The purity of the fluorination products was analysed by X-ray diffraction (XRD) and differential scanning calorimetry (DSC) methods.

A specially designed facility installed recently in JRC-Karlsruhe for synthesis of pure actinide fluorides using pure HF gas at elevated temperatures is described in detail. The experimental set-up consists of a glove box kept under a purified argon atmosphere, a high temperature horizontal fluorination reactor and a HF supply gas line connected to the glove box. The facility is unique in that it enables synthesis of highly radioactive actinide fluorides, such as plutonium and americium, in a gram scale and using pure HF gas. The present work served not only for preparation of pure UF_4 and ThF_4, but also for verification and optimisation of the fluorination procedures and set-up for the future work with transuranium elements.

2. Literature survey on the UF_4 and ThF_4 synthesis

The hydrofluorination of UO_2 as a method for synthesis of UF_4 was studied by many authors. Katz and Rabinowitch [12] in their work from early 1950's recommend synthesis of UF_4 by reaction of UO_2 with gaseous fluorination agents at elevated temperatures. They especially highlighted the reaction with HF gas, as this method is distinguished by simplicity of procedure and the relative ease with which a pure anhydrous product can be prepared. They also stated that this reaction is however relatively slow and the reaction rate does not depend on temperature above 350°C.

Tomlinson [13] published in 1961 a study on kinetics of this reaction in temperature range 200-450°C, showing that the reaction rate is dependent on the surface area of the UO_2 powder. He observed a limiting surface area is 2.1 m^2/g, as above this value the rate remained constant. This work was followed by other kinetics studies, e.g., Dell [14] studied in detail the conversion of UO_3 to UO_2 by reduction using H_2 gas at temperatures 520-620°C and successive conversion of the formed UO_2 to UF_4 by hydrofluorination at 450°C, Ellis [15] evaluated the reaction rates of the formation of UF_4 interference films on an UO_2 polished surface at temperatures 200-300°C and Nicole [16] studied the transformation of UO_2 to

UF_4 by hydrofluorination with the aid of thermogravimetric experiments performed at temperatures from 220 to 450°C in a nitrogen-diluted HF atmosphere. The reaction kinetics was found to be of the first order with respect to hydrogen fluoride, with an activation energy of 25 kJ/mol.

Other works devoted to the preparation of pure UF_4 were published e.g. by Eykens [17] and Kim [18]. Eykens carried the hydrofluorination in a flow-through furnace at 550-600°C and used UO_2 prepared by different methods. The preferred initial material was obtained via the oxalate calcination at 450°C, while the required temperature for fluorination was 600°C. The reaction was complete after 35 minutes fluorinating of 0.1-1.0 g of the oxide. However, no analytical results proving the purity of the prepared UF_4 were shown. Kim studied synthesis of UF_4 both in a fluoride melt (LiF-BeF_2 eutectic mixture) and as a solid state - gas reaction at a temperature of 550°C. As a fluorination agent, HF gas mixed with H_2 was used to reduce possibly present UO_3. As one of the results it was shown that due to the very low solubility of HF gas in the molten fluoride salt, hydrofluorination by gas-solid reaction was far more effective than that in the molten fluoride salt.

Significantly less data were published on the synthesis of ThF_4. Several possible methods were mentioned in the literature, e.g. by Fisher [19], including hydrofluorination of ThO_2 at elevated temperature. Wani [20] prepared ThF_4 by mixing NH_4HF_2 with ThO_2 at room temperature. A kinetic study on the hydrofluorination of ThO_2 was carried out by Lindstrom [21] and uniform interference films of ThF_4 were achieved in this study on the single crystals of ThO_2 by reaction with gaseous HF at six temperatures in the interval 218-327°C. In a previous work published by Souček at al. [22], which was mainly dealing with electrochemistry of actinides in molten fluoride salt, ThF_4 was prepared by direct hydrofluorination of ThO_2 at a temperature of 650°C as a gas-solid reaction in the flow of HF gas. Although the purity of the product enabled the electrochemical measurements, it was not pure enough for thermodynamic characterisation, as shown by DSC analysis.

3. Experimental

Pure UF_4 and ThF_4 were synthesised from the respective oxides for further thermodynamic and electrochemical characterisation. The work was carried out using a facility for hydrofluorination of actinides described below. All chemicals and samples were stored and treated in a glove-box under a pure Ar atmosphere with oxygen and moisture content less than 1 ppm. The experimental parameters were set on the basis of thermodynamic calculations presented in section 4.1 and the products were characterised by XRD and DSC techniques. Furthermore, re-assessment of UF_4 melting point using a very pure sample was achieved.

3.1 Installation for hydrofluorination of actinides

The installation for hydrofluorination of actinides was originally designed and installed at JRC-Karlsruhe in 2013 and it consists of two connected glove boxes, a high temperature fluorination reactor and a HF supply gas line connected to the main glove box.

The main glove box is kept under pure Ar gas atmosphere to avoid any non-desired reactions of the fluorinated material with moisture and oxygen from the ambient atmosphere. The Ar gas is constantly purified and the system is controlled to keep the concentration of H_2O and O_2 inside the glove box less than 5 ppm, while the real measured values are typically below 1 ppm. The windows of the box are made of polycarbonate and gloves are double-layered from Hypalon and Neoprene to withstand aggressive chemicals and minimise oxygen diffusion. The main equipment of the box comprises a high precision balance, a water-cooling system and the below detailed fluorination reactor and HF gas line connection. The main Ar glove box is connected to an auxiliary glove box via an antechamber, which can be flushed by purified Ar gas. The adjacent box is operated under nitrogen atmosphere and serves for introducing and removal of the material as well as for supporting works, e.g., cleaning of the equipment or preparation of samples non-sensitive to moisture and oxygen. A photo of the glove boxes with the installed equipment is shown in Fig. 1.

3.2 Fluorination apparatus

The fluorination apparatus consists of a horizontal tube reactor inserted in a resistance furnace enabling work at temperatures up to 1200°C. A scheme of the device with the description of the main parts is shown in Fig. 2. The reactor is intended for a solid-gas reaction and the starting powdered material is inserted in a boat to the homogeneous heating zone in the centre of the tube (length approximately 60 mm) via supporting rails welded to the inner wall of the tube. The boat made of Inconel X750 has dimensions 50 x 50 x 10 mm enabling batch up to 10 g of the initial material. The powder stays in the boat during the complete fluorination.

The main body of the reactor is a tube with a volume approximately 1 l and it is hermetically closed on both sides by water-cooled removable flanges. One flange is equipped with three gas inlet ports, a HF resistant pressure sensor WIKA S-10 high-quality pressure transmitter mounted in a specially designed holder from Inconel X750 and a thermocouple sheath, while the gas outlet is on the second flange. The design thus allows operation under static conditions or flow-through fluorination. In the static conditions, the reactor can be evacuated using a membrane vacuum pump to the absolute pressure 1 mbar and filled with pure HF gas. In dynamic conditions, the HF gas can be led directly above the boat filled with the powder while the non-reacted gas and the formed gaseous products are removed to the off-gas unit consisting of HF gas commercially acquired absorber and HF gas detector. In addition, an inert carrier gas or second reactive gas can be led into the reactor. The material of all metallic components of the reactor which are in contact with HF gas is a heat resistant stainless steel AISI 314 / 1.4841 having very good resistance to corrosion. The gaskets are made from resistant PTFE, since they are at places cooled by water-cooling rings.

3.3 HF gas supply

The HF gas line consists of a main gas supply unit including the HF and Ar gas cylinders, a connection piping, a HF off-gas absorber and a computer controlled panel. The gas- supply unit, installed in a special safety cupboard, is shown in Fig. 3. The operation is partly automatic using Lab-View based software, while the gas flow rate is provided by a mass flow controller unit. The piping for HF gas was made from double-wall, electro-polished stainless steel with welds controlled by radiography and monitored for leakage. HF gas sensors, mounted inside the safety cupboard, inside the glove box and in the laboratory are part of the continuous gas detection system for personal security during the fluorination experiments. An automatic shutdown procedure using a pneumatic electro valve installed on the HF gas cylinder is applied in case of HF detection, followed by automatic flushing of the line by Ar gas through the HF absorbers. The complete line, including the valves and mass flow controller, is heated to 40°C, i.e., well above the HF boiling point of 19.5°C, to prevent HF condensation.

3.4 Preparation of the initial materials

In order to enhance the kinetics of the fluorination reaction, a special attention was paid to the preparation of the initial oxide material. The powder should have the highest possible surface to increase the reactivity and especially in case of uranium, a stoichiometric UO_2 was needed because otherwise a mixture of uranium fluorides of different oxidation states was achieved (unpublished results of preliminary experiments). The first step of the procedure for preparation of UO_2 consisted of electrochemical reduction of U(VI) to U(IV) from nitrate solution in presence of hydrazine using a platinum cathode. The anode was introduced in a tube with porous sintered glass end to prevent back oxidation of uranium, while insuring the ionic conduction. This method is very similar to the original work on synthesis of nano-sized particle UO_2 as published in [23]. The electrochemical reduction was followed by precipitation of U(IV) by oxalic acid, filtration of the formed oxalate and its thermal decomposition and conversion to oxide at 800°C for 4 hours under dynamic Ar/H_2 atmosphere.

In case of thorium, the procedure was analogous, but without necessity of the reduction as the Th(IV) nitrate solution was directly available. After the precipitation, the conversion to oxide was done at the same temperature, but using a dynamic air atmosphere. At such calcination temperature and time, the oxalate decomposition yields an oxide powder with surface area of approximately 10-15 m^2/g [24] and in the same time it enables efficient removal of the carbonates and moisture adsorbed on the oxide powders from the preparation process. The procedure and characterisation of UO_2 and ThO_2 prepared by analogous methods is described in detail in [25]. Both initial nitrate solutions were from the stock of JRC-Karlsuhe.

The thus prepared oxides were measured by XRD and the successive Rietveld analyses confirmed presence of pure and stoichiometric UO_2 and ThO_2 phases. The XRD patterns of both materials are shown in Fig. 4. The evaluation of the crystal size using Williamson-Hall method gave 140 and 30 nm for UO_2 and ThO_2, respectively.

3.5 Procedures for the UF_4 and ThF_4 syntheses

The applied syntheses is based on solid-gas reactions between the stoichiometric UO_2 and ThO_2 fine powders (oxygen/metal ratio set to 2.00) with pure HF gas at elevated temperatures according to the reaction equations (1) and (2), respectively:

$$UO_2(s) + 4HF(g) \rightarrow UF_4(s) + 2H_2O(g) \tag{1}$$

$$ThO_2(s) + 4HF(g) \rightarrow ThF_4(s) + 2H_2O(g) \tag{2}$$

The powder was inserted into the Inconel boat in several batches from 1 to 5 grams and placed in the central homogeneous heating zone of the horizontal fluorination reactor (see section 3.2 above). The reactor was gas tight-closed, evacuated to an absolute pressure of 1 mbar and heated to the desired temperature, which was estimated from the thermodynamic calculations described below in section 4.1. HF gas was then slowly introduced into the reactor and after reaching a slight overpressure of 1.05 bar, HF gas was flushed through the reactor to the off gas treatment absorber. The overall HF gas molar excess over the reaction stoichiometry was usually 3-4. The typical parameters for both reactions are summarised in Table 1.

3.6 Analytical techniques

The synthesised ThF_4 and UF_4 were analysed by X-ray diffraction for the qualitative phase analysis followed by Rietveld refinement and by DSC for the melting temperature determination.

The XRD samples were prepared by embedding of approximately 75 mg product powder into a resin, while the powder was beforehand homogenised by manual grinding in an agate mortar. The XRD measurements were carried out using a Bruker D8 Bragg-Brentano Advance diffractometer (Cu Kα1 radiation) equipped with a LynxEye Linear Position Sensitive detector. The operation conditions were 40 kV and 40 mA. Powder diffraction patterns were recorded at room temperature across an angular range $20° \leq 2\theta \leq 110°$. The phase quantification procedure involved in the identification of the different phases was done using Jana 2006 crystallographic software [26]. Atomic positions of fluorides phases have not been refined and have been fixed based on values of Kern [27] obtained through neutron diffraction. The Rieltveld refinement was done for each sample to confirm that the synthesised fluorides yielded XRD patterns in agreement with the published structures.

The detection limit of a phase in XRD depends on many parameters, e.g., acquisition time, crystallinity or symmetry of the phases and amount of the sample. In the present case, the method was used mainly to determine if highly crystalline UO_2 or ThO_2 is present in the relatively low crystalline UF_4 or ThF_4. In addition, UO_2 and ThO_2 have their most intensive diffraction peak at 28.2° 2θ, where the fluorides have no diffraction, long acquisition time of 8 h was used and about 70 mg of the samples were measured. Therefore it was concluded that in the given case, the detection limit of XRD for the oxide phases was <1 wt.%.

Other technique that was employed in this study for verification of the sample's purity was a melting point determination by differential scanning calorimetry (DSC). This method is well recognized as one of the most sensitive techniques to determine whether substantial quantities of any impurities are present in the sample. The apparatus used in this study was a Setaram multi detector high temperature MDHTC-96 type calorimeter with installed DSC detector based on S-type thermocouples with peak temperature of 1400 °C. The program for melting temperature determination consisted of two heating and two consecutive cooling ramps of a rate 10 K/min and a temperature range from room temperature to 1250 °C, well above melting points of UF_4 and ThF_4. To avoid evaporation of fluoride samples at high temperature, both materials have been encapsulated in gas tight, high pressure resistant stainless steel crucibles with inserted nickel liners to prevent any undesired reaction between fluoride salt and the steel. For more details about the encapsulation technique used in this work we refer to our earlier paper by Beneš et al. [28]. To prevent oxidation of the steel container, an argon atmosphere was used during the measurement. Prior to experiment the calorimeter was calibrated by series of standard materials (In, Sn, Zn, Pb, Al, Ag, Au) of different melting points, placed in the same crucibles to correct for the offset temperature during the measurement. The uncertainty of the measurements was determined as ±3 °C.

4. Results and discussion

4.1 Thermodynamic calculations

To estimate the optimal experimental conditions, thermodynamic calculations were carried out using the commercial FactSage software with integrated pure substances database taken from HSC Chemistry 6.12 (Outotec Research Oy, Finland). The calculations were based on the Gibbs energy minimisation method and the products of the hydrofluorination reactions were predicted by calculating the equilibrium compositions of the given mixtures in dependency on temperature. The real parameters of the available experimental set-up were taken into account when defining the calculation conditions, which included total pressure of the system set to 1 bar containing the equilibrium gas mixture of HF with the formed H_2O.

Fig. 5 shows the results of the equilibrium compositions of the products for fluorination of UO_2 and ThO_2 as a function of the temperature, computed for initial weights of oxides equal to 5 grams. The main expected products are solid UF_4, resp. ThF_4, however at the given conditions at elevated temperatures, recombination of the formed water would lead to formation of oxyfluorides and at yet higher temperatures even to oxide. It is valid especially when assuming the experimental procedure utilising a closed system when filling the evacuated reactor with pure HF gas without removal of the formed by-products, as described in section 3.5. Therefore, the maximum thermodynamically acceptable temperatures were selected to enhance the reaction kinetics, but avoiding this possible unwanted recombination reaction.

4.2 Characteristics of the products

A dark green powder was obtained in case of UF_4 product, while ThF_4 was white with a light shadow shade. Both colours agree with the reported appearance of the respective fluorides. The dark shade of the green colour was likely reached due to rather small particle size of the initial and thus also the final powders. The photos of both initial materials and the products are shown in Fig. 6. For the colour photos, please refer to the online version of the article. The gravimetric mass balances indicated very high conversion efficiencies for both reactions with a yield typically around 99.6%, while the deviation from ideal mass is likely due to possible losses during manipulations in the glove box and/or due to weighing error.

In case of UO_2 fluorination, two consequent runs had to be performed to achieve a pure product, free from any residual oxide. The powder after the first run was homogenised by manual grinding in a mortar, refilled to the boat and the process was repeated using the same conditions. For ThO_2, one fluorination run was sufficient to obtain fully oxygen free product. The possible explanation can be the 4 times larger particle size of UO_2 in comparison to the ThO_2 initial material (see section 3.4) and/or the lower reaction temperature for UO_2 fluorination based on the thermodynamic calculation of the equilibrium composition as a function of the temperature (see section 4.1). Both factors likely lead to to slower kinetics of the UO_2 fluorination.

4.3 X-ray diffraction analysis

The typical XRD diffractogram of the product of UO_2 fluorination is shown in Fig. 7. The main black pattern shows a single phase UF_4 after the two fluorination runs. The detail on the inset in the right upper corner of the figure shows a comparison of the patterns from 26° to 32° 2θ obtained after first and second runs of the fluorination. UO_2 has the most intensive diffraction peak at 28.2° 2θ, while UF_4 has no peaks in this region. Therefore, it is the most significant region for detection of possible traces of UO_2 in the product. The figure shows that after the first fluorination, the conversion was not fully completed and the second run was needed. This phenomenon was observed for all samples. The Rietveld refinement of the pattern after first fluorination gave a UO_2 proportion of about 1 wt.% in the powder. After the second run, no indication of UO_2 traces was observed.

The analysis of the product of ThO_2 fluorination revealed an efficient conversion already after a single reaction step. The respective XRD diffractogram, shown in Fig. 8, contains only the pattern of single phase ThF_4. The results of the Rietveld refinement for both products are summarised in Table 2. In case of UF_4, the difference between experimental and calculated profiles is relatively important, which is likely caused by an anisotropic broadening, which makes profile fitting difficult. Apart from that, intensities from calculated structure are in a fair agreement in both cases

4.4 Differential scanning calorimetry analysis

Conventional differential scanning calorimetry was used for the melting temperature determination, which is a significant indicator of purity. The melting temperature determinations of both fluorination products are shown in Fig. 9. For the product of UO_2 fluorination, the measured melting temperature was found at 1034.7 (±3.0)°C, which is only slightly lower compared to the literature value 1036°C and falls into the uncertainty of the measurement. However, the published melting point is a value extrapolated by Sheil [29] and corrected for UO_2 impurities, and not obtained by direct characterisation of pure UF_4. Since the XRD analysis performed in this study did not reveal any impurities and the DSC curve showed clearly single peak upon melting point, which indicated purity of the sample >99 wt.%, we suggest 1034.7 (±3)°C as a novel determined melting point of UF_4. In case of ThF_4, the measured melting temperature of purified material was found at 1111.4 (±3)°C, which is also in a very good agreement with the literature value 1110.0 °C [30].

5. Conclusion

The fluorination of UO_2 and ThO_2 powders with high specific surface area by pure HF gas at temperatures of 450°C and 600°C, respectively, has led to pure solid UF_4 and ThF_4. The purity has been verified by XRD phase analyses in a combination with conventional DSC melting temperature determination. For the first time, the melting point of UF_4 was determined directly by a calorimetric technique on a phase pure sample (>99%) and was found at 1034.7 (±3)°C. This work has demonstrated the feasibility of the proposed syntheses to prepare very pure actinide fluorides for thermodynamic and electrochemical characterisation, which is a very important step for the molten salt reactor fuel cycle safety assessment. At the same time, the functionality and satisfactory efficiency and reliability of the installed fluorination facility in JRC-Karlsruhe has been shown and the analytical scheme has been established. Therefore, the work will continue by syntheses of transuranium actinide fluorides.

Acknowledgement

The authors wish to thank G. Nagel and V. Ernst for design of the fluorination reactor, K. Thellmann and C. Gastager from the company LOGITEX Reinstmedientechnik GmbH for the design, installation and a great help with starting of the operation of the HF gas supply unit, A. Rodrigues for experimental support, Eckhard Dahms and Daniel Bouexière for XRD analyses and many other colleagues from JRC-Karlsruhe for help and valuable discussions. This work was carried out with the European Commission financial support in the Horizon 2020 framework program, under the collaborative project "SAMOFAR", grant agreement number 661891 — SAMOFAR: A Paradigm Shift in Nuclear Reactor Safety with the Molten Salt Fast Reactor.

References

[1] H.G. MacPherson, The Molten Salt Reactor Adventure, Nucl. Sci. Eng. 90 (1985) 374–380.

[2] M.W. Rosenthal, P.R. Kasten, R.B. Briggs, Molten-salt reactors - history, status, and potential, Nucl. Technol. 8(2) (1970) 107-117.

[3] J. Serp, M. Alibert, O. Beneš, S. Delpech, O. Feynberg, V. Ghetta, D. Heuer, D. Holcomb, V. Ignatiev, J.L. Kloosterman, L. Luzzi, E. Merle-Lucotte, J. Uhlíř, R. Yoshioka, D. Zhimin, The molten salt reactor (MSR) in generation IV: Overview and perspectives, Prog. Nucl. Energ. 77 (2014) 308–319.

[4] Technology Roadmap Update for Generation IV Nuclear Energy Systems, Generation IV International Forum, OECD Nuclear Energy Agency, January 2014, pp. www.gen-4.org.

[5] H. Xu, China's TMSR programme, Workshop on Molten Salt Reactor Technologies - Commemorating the 50th Anniversary of the Startup of the MSRE - From the MSRE to a New Emerging Class of Reactors 50 Years Later, ORNL, USA, 2015.

[6] Accelerator-Driven Sub-Critical Molten Salt Reactor (ADSCMSR), http://egeneration.org/solution/adscmsr-accelerator-driven-sub-critical-molten-salt-reactor/, access date 05/2017.

[7] S.B. Degweker, P. Singh, P. Satyamurthy , A. Sinha, Accelerator Driven Systems for Thorium Utilisation in India, International Thorium Energy Conference, Geneva, Switzerland, 2013.

[8] I. Slessarev, V. Berthou, M. Salvatores, A. Tchistiakov, Concept of the thorium fuelled accelerator driven subcritical system for both energy production and TRU incineration - 'TASSE', ADTTA '99 - 3rd international conference on accelerator driven transmutation techniques and applications, Prague, Czech Republic, 1999.

[9] V. Ignatiev, O. Feynberg, I. Gnidoi, A. Merzlyakov, A. Surenkov, V. Uglov, A. Zagnitko, V. Subbotin, I. Sannikov, A. Toropov, V. Afonichkin, A. Bovet, V. Khokhlov, V. Shishkin, M. Kormilitsyn, A. Lizin, A. Osipenko, Molten salt actinide recycler and transforming

system without and with Th–U support: Fuel cycle flexibility and key material properties, Ann. Nucl. Energy 64 (2014) 408–420.

[10] M. Brovchenko, D. Heuer, E. Merle-Lucotte, M. Allibert, V. Ghetta, A. Laureau, P. Rubiolo, Design-Related Studies for the Preliminary Safety Assessment of the Molten Salt Fast Reactor, Nucl. Sci. Eng. 175(3) (2013) 329-339.

[11] S. Delpech, E. Merle-Lucotte, D. Heuer, M. Allibert, V. Ghetta, C. Le-Brun, X. Doligez, G. Picard, Reactor physic and reprocessing scheme for innovative molten salt reactor system, J. Fluorine Chem. 130(1) (2009) 11-17.

[12] J.J. Katz, E. Rabinowitch, The Chemistry of Uranium Part I. , McGraw-Hill Book Company Inc., New York-Toronto-London, 1951.

[13] L. Tomlinson, S.A. Morrow, S. Graves, Kinetics of the hydrofluorination of uranium dioxide, Trans. Faraday Soc. 57 (1961) 1008-1018.

[14] R.M. Dell, V.J. Wheeler, Chemical reactivity of uranium trioxide. Part 1. - Conversion to U_3O_8, UO_2 and UF_4, Trans. Faraday Soc. 58 (1962) 1590-1607.

[15] W.P. Ellis, Hydrofluorination kinetics of doped uranium dioxide, J. Nucl. Mater. 19(2) (1966) 212-214.

[16] C. Nicole, F. Patisson, D. Ablitzer, J.L. Houzelot, A thermogravimetric study of the kinetics of hydrofluorination of uranium dioxide, Chem. Eng. Sci. 51(23) (1996) 5213-5222.

[17] R. Eykens, J. Pauwels, J. Van Audenhove, The hydrofluorination of uranium and plutonium, Nucl. Instrum. Meth. A 236(3) (1985) 497-499.

[18] E.H. Kim, S.W. Kwon, D.S. Hwang, W.M. Cheong, J.H. Park, J.H. Yoo, Fluorination of UO_2 and CeO_2 under the atmosphere of HF and H2, J. Ind. Eng. Chem. 8(1) (2002) 98-102.

[19] R.W. Fisher, The Preparation of Thorium Oxide and Thorium Fluoride from Thorium Nitrate, Pergamon Press, London, 1958.

[20] B.N. Wani, S.J. Patwe, U.R.K. Rao, K.S. Venkateswarlu, Fluorination of oxides of uranium and thorium by ammonium hydrogenfluoride, J. Fluorine Chem. 44(2) (1989) 177-185.

[21] R.M. Lindstrom, W.P. Ellis, Kinetics of the Hydrofluorination of Thorium Dioxide, The J. Chem. Phys. 43(3) (1965) 994-997.

[22] P. Souček, F. Lisý, R. Tuláčková, J. Uhlíř, R. Mráz, Development of Electrochemical Separation Methods in Molten LiF-NaF-KF for the Molten Salt Reactor Fuel Cycle, J. Nucl. Sci. Technol. 42(12) (2005) 1017-1024.

[23] R. Jovani-Abril, M. Gibilaro, A. Janßen, R. Eloirdi, J. Somers, J. Spino, R. Malmbeck, Synthesis of nc-UO_2 by controlled precipitation in aqueous phase, J. Nucl. Mater. 477 (2016) 298-304.

[24] N. Hingant, N. Clavier, N. Dacheux, S. Hubert, N. Barré, R. Podor, L. Aranda, Preparation of morphology controlled $Th_{1-x}U_xO_2$ sintered pellets from low-temperature precursors, Powder Technol. 208(2) (2011) 454-460.

[25] V. Tyrpekl, J.F. Vigier, D. Manara, T. Wiss, O. Dieste Blanco, J. Somers, Low temperature decomposition of U(IV) and Th(IV) oxalates to nanograined oxide powders, J. Nucl. Mater. 460 (2015) 200-208.

[26] V. Petříček, M. Dušek, L. Palatinus, Crystallographic computing system JANA2006: General features, Z. Kristallogr. 229 (2014) 345-352

[27] S. Kern, J. Hayward, S. Roberts, J.W.R. Jr., F.J. Rotella, L. Soderholm, B. Cort, M. Tinkle, M. West, D. Hoisington, G.H. Lander, Temperature variation of the structural parameters in actinide tetrafluorides, J. Chem. Phys. 101(11) (1994) 9333-9337.

[28] O. Beneš, R.J.M. Konings, S. Wurzer, M. Sierig, A. Dockendorf, A DSC study of the $NaNO_3$-KNO_3 system using an innovative encapsulation technique, Thermochim. Acta 509 (2010) 62-66.

[29] R.J. Sheil, The system UF_4-UO_2, The system UF_4-UO_2 in ORNL-2061 (1956) 71.

[30] M. Rand, J. Fuger, I. Grenthe, V. Neck, D. Raiof, Chemical thermodynamics of Thorium, Vol. 11. Chemical Thermodynamics Series, OECD Nuclear Energy Agency, Data Bank, Issy-les-Moulineaux, France (2009) 198.

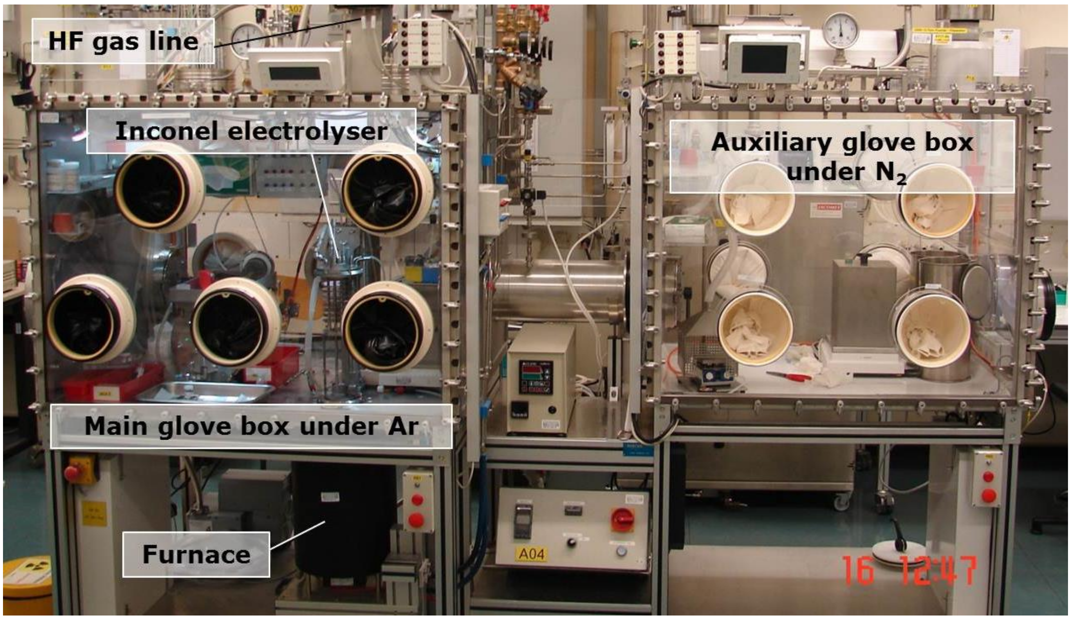

Fig. 1 *Glove boxes for synthesis of pure actinide fluorides and electrochemistry in molten fluoride salts connected to a HF gas line*

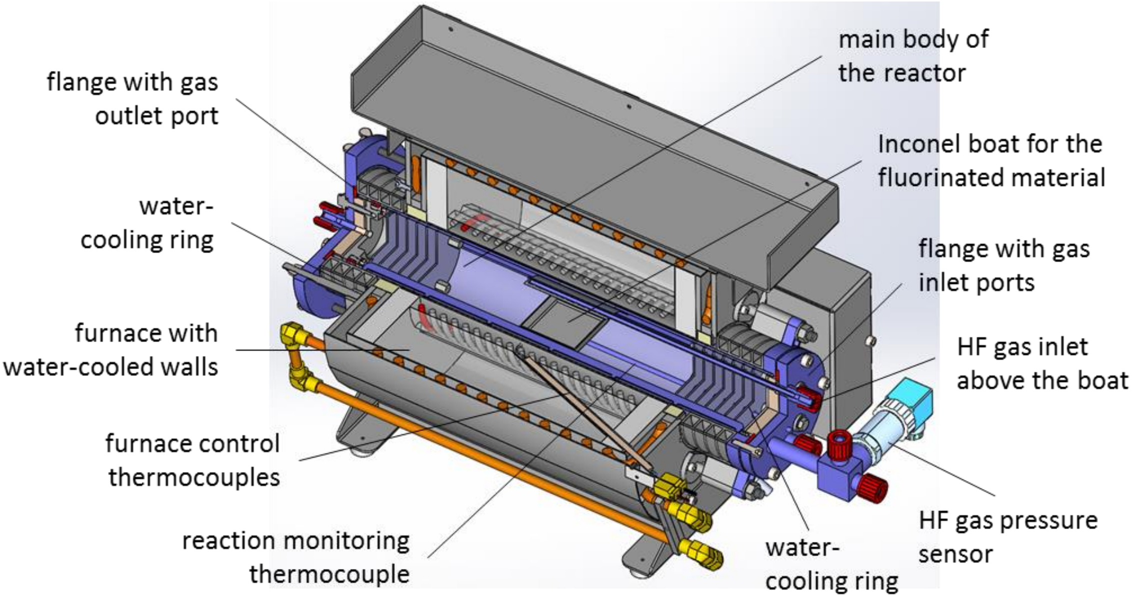

Fig. 2 *Scheme of the fluorination reactor inserted in the resistance horizontal furnace*

Fig. 3 *HF gas main supply unit installed in a safety cupboard*

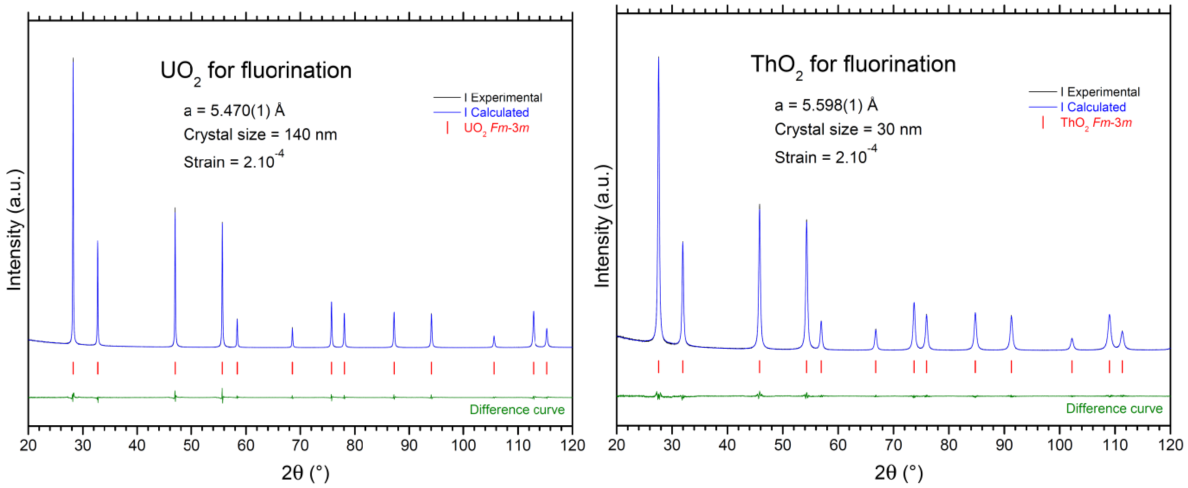

Fig. 4 *XRD patterns of UO_2 (left) and ThO_2 (right) initial material for fluorination*

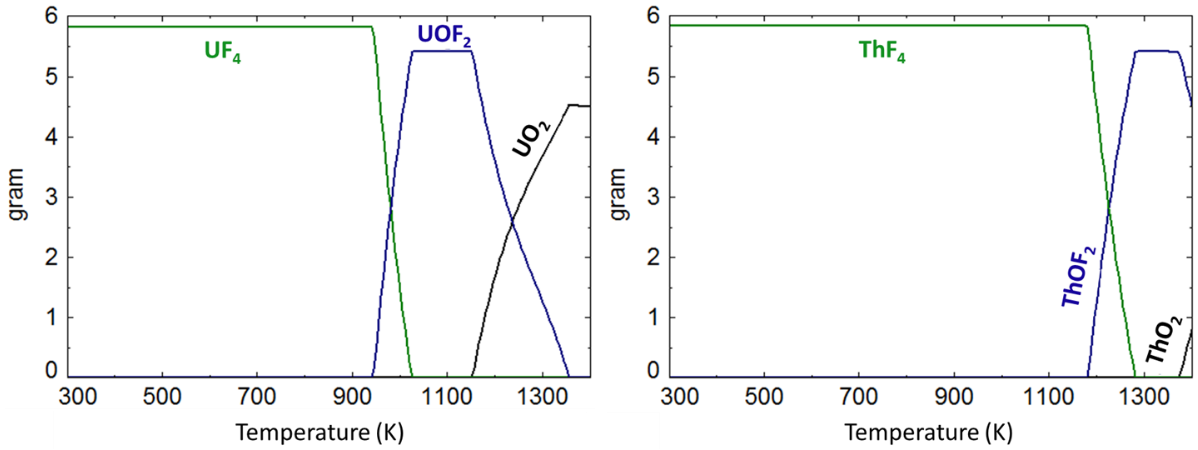

Fig. 5 *Calculated equilibrium composition of the products for fluorination of* UO_2 *(left) and* ThO_2 *(right) by pure HF gas in dependency on the temperature (*H_2O *and the excess of HF gas are not shown)*

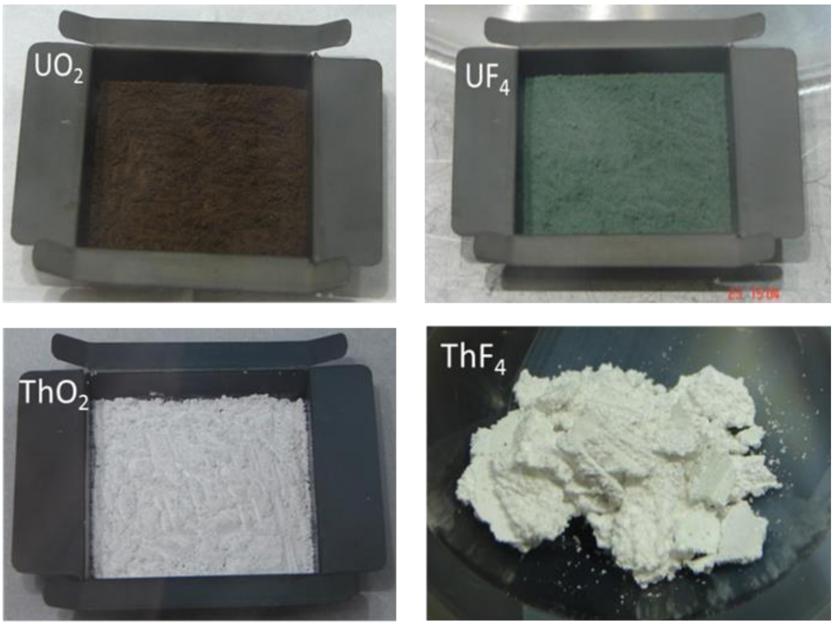

Fig. 6 *Photos of the initial materials* UO_2 *(up left) and* ThO_2 *(down left) and final products* UF_4 *(up right) and* ThF_4 *(down right). For the colour photos, please refer to the online version of the article.*

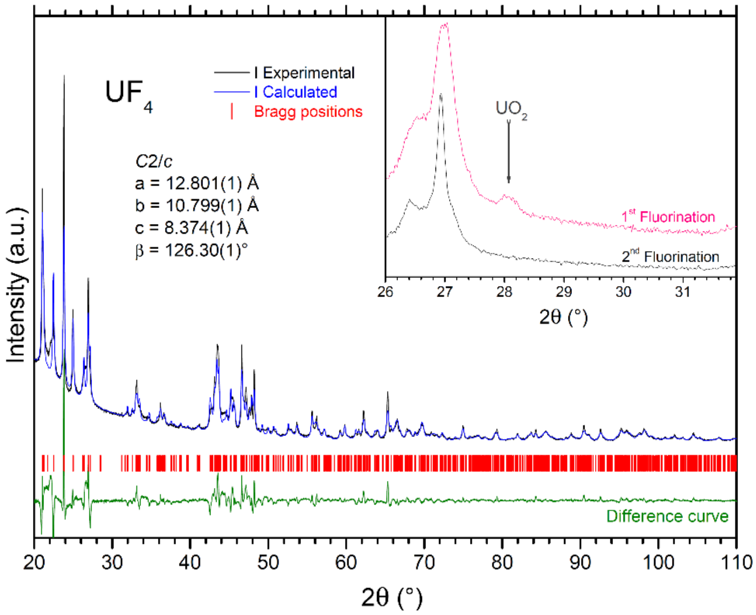

Fig. 7 *Rietveld refinement of XRD pattern obtained after the second* UO_2 *fluorination. The inset shows XRD experimental pattern obtained after the 1st and 2nd reaction steps.*

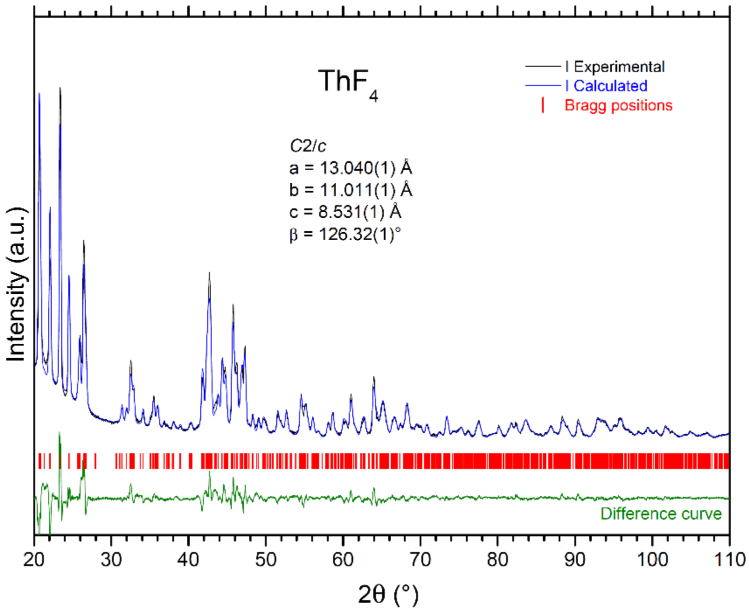

Fig. 8 *XRD Rietveld refinement of the product of ThO_2 fluorination*

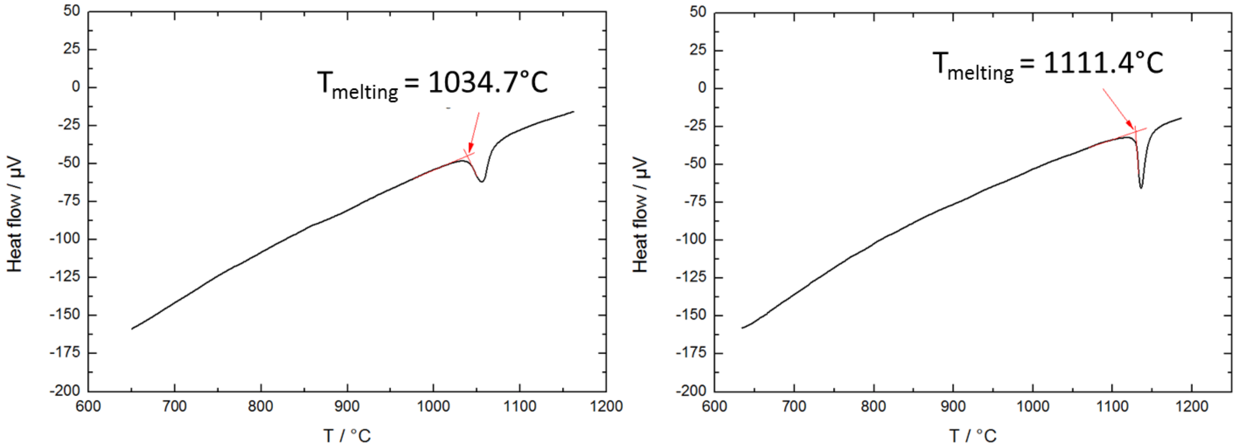

Fig. 9 *Melting temperature determinations of UF_4 (left) and ThF_4 (right) by DSC*

Table 1 *Process parameters for fluorinations of UO_2 and ThO_2*

Process step/parameter	UO_2	ThO_2
Temperature	450°C	600°C
Filling of the reactor	50 ml/min, 20 – 60 min, depending on the reaction kinetics and possible corrosion reactions with the construction material	
Flushing through	50 ml/min, 20 – 140 minutes according to the oxide mass	
HF excess removal	Ar flow, 50 ml/min, min. 240 min while cooling down	

Table 2 *Results of the Rietveld refinement of fluorinations products*

Parameter / product	UF_4	ThF_4
Space group	*C2/c*	*C2/c*
R_p (%)	7.89	5.08
R_{wp} (%)	11.20	7.00
a (Å)	12.801(1)	13.040(1)
b (Å)	10.799(1)	11.011(1)
c (Å)	8.374(1)	8.531(1)
β (°)	126.30(1)	126.32(1)
V (Å^3)	932.9(1)	986.9(1)